FEBS Letters

FEBS PRESS science publishing by scientists

REVIEW

Fluorescence CLEM in biology: historic developments and current super-resolution applications

Koen van den Dries[1], Jack Fransen[1,2] and Alessandra Cambi[1]

1 Department of Cell Biology, Radboud Institute for Molecular Life Sciences, Radboudumc, Nijmegen, The Netherlands
2 Microscopic Imaging Center, Radboud Institute for Molecular Life Sciences, Radboudumc, Nijmegen, The Netherlands

Correspondence
A. Cambi, Department of Cell Biology, Radboud Institute for Molecular Life Sciences, Radboudumc, Route 283 Cell Biology, Geert Grooteplein 26/28, 6525 GA Nijmegen, The Netherlands
Tel: +31 (0)24 361 43 29
E-mail: alessandra.cambi@radboudumc.nl

(Received 14 February 2022, revised 24 May 2022, accepted 25 May 2022, available online 17 June 2022)

doi:10.1002/1873-3468.14421

Edited by Jan Borst

Correlative light and electron microscopy (CLEM) is a powerful imaging approach that allows the direct correlation of information obtained on a light and an electron microscope. There is a growing interest in the application of CLEM in biology, mainly attributable to technical advances in field of fluorescence microscopy in the past two decades. In this review, we summarize the important developments in CLEM for biological applications, focusing on the combination of fluorescence microscopy and electron microscopy. We first provide a brief overview of the early days of fluorescence CLEM usage starting with the initial rise in the late 1970s and the subsequent optimization of CLEM workflows during the following two decades. Next, we describe how the engineering of fluorescent proteins and the development of super-resolution fluorescence microscopy have significantly renewed the interest in CLEM resulting in the present application of fluorescence CLEM in many different areas of cellular and molecular biology. Lastly, we present the promises and challenges for the future of fluorescence CLEM discussing novel workflows, probe development and quantification possibilities.

Keywords: cell biology; correlative microscopy; electron microscopy; fluorescence; fluorescent proteins; light microscopy; super-resolution microscopy

Correlative light and electron microscopy (CLEM) is the general term used to describe techniques that allow combining the information from images acquired on a light and an electron microscope. CLEM is a powerful imaging approach that, due to the fact that electrons have a much shorter wavelength compared to photons, offers the possibility to collect different types of data from a biological sample. In the past decades, many different CLEM approaches have been developed. Yet, most of the recently published work uses fluorescence as the light microscopy readout, for this review, we focus on the combination of fluorescence microscopy (FM) and electron microscopy (EM). As such, we specifically discuss the correlation between fluorescence and electron images of the same area of a given biological sample. By performing such a correlation, the FM images allow researchers to observe the localization of one or more molecules of interest, while the EM images provide the corresponding ultrastructural context. In this review, we first provide a historic timeline of the early developments in fluorescence CLEM. Next, we present the major advances in CLEM achieved since

Abbreviations
CLEM, correlative light and electron microscopy; EM, electron microscopy; FIB, focused ion beam; FM, fluorescence microscopy; FP, fluorescent protein; iPALM, interferometric photoactivated localization microscopy; OSSM, oxygen serial spin mill; PALM, photoactivated localization microscopy; SEM, scanning electron microscopy; SR, super-resolution; STED, stimulated emission depletion; STORM, stochastic optical reconstruction microscopy; TEM, transmission electron microscopy.

FEBS Letters **596** (2022) 2486–2496

the early 2000s and describe the current state-of-the-art approaches. Finally, we discuss the future opportunities and challenges of fluorescence CLEM in biology.

Historic timeline

Early days

Almost parallel to the first applications of FM and EM for biological samples that emerged in the 60s and 70s of the 20th century, there have been attempts to combine these two approaches (Fig. 1). The first fluorescence CLEM reports were published in the mid to late 1970s. In these early works, CLEM was primarily used to confirm the identity of cells or cellular substructures which could not have been done by either FM or EM alone. With only very few specific antibodies available for FM, the probes used for the identification of cells or subcellular structures included general compounds such as serum IgGs to separate macrophages from tumour cells [1] or small fluorescent DNA-binding probes to localize the nucleus in lymphocytes [2]. Interestingly, fluorescence CLEM also proved valuable for the development of novel antibodies against, for example, the cytoskeletal protein tubulin [3]. Ultrastructural information from EM was used to confirm the specificity and the applicability of this antibody for FM studies [3]. While these early examples demonstrate the initial value of CLEM, biological information was only obtained from either the FM or EM micrographs.

The first examples of studies that truly exploit CLEM to derive different types of biological information from the same sample include work on spreading macrophages [4] and white blood cells [5]. In spreading macrophages, FM was used to demonstrate the existence of actin-rich structures while the EM was used to resolve actin fibres that connect these structures, something which could not be resolved by FM alone at the time [4]. For the white blood cells, FM was applied to measure the cellular DNA content to establish ploidy or cell cycle stage, which was correlated with the ultrastructure of different blood cell types in EM. In later studies, the discovery that the fluorescence from fluorescein isothiocyanate was preserved after Epon resin embedding was exploited to correlate FM with EM within the same tissue section [6]. This resulted in a variety of studies including the localization of actinin and titin within the ultrastructure of myofibrils in chick embryos [7] as well as the microtubule organization in unicellular protozoans [8,9].

1990s—Early 2000s

The early developments of CLEM have only been followed up by a few in the 1990s. For example, the group of Borisy recognized that CLEM would be ideal to study membrane-associated cytoskeletal elements. They developed a workflow in which FM was used to observe fluorescently labelled myosin injected in living cells, which was correlated with platinum replica EM images of ventral plasma membrane preparations [10].

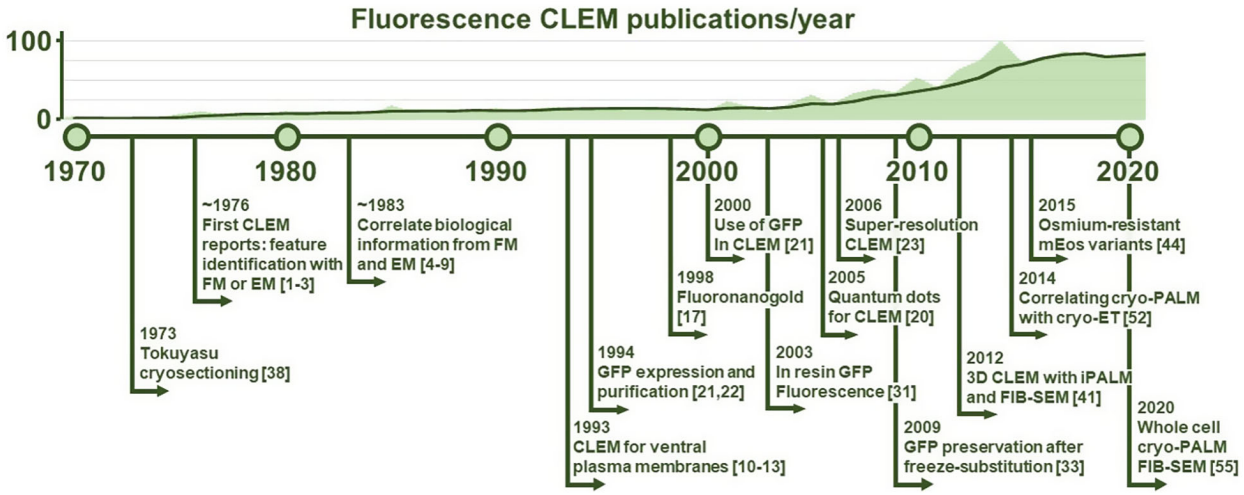

Fig. 1. Historic timeline of developments in fluorescence CLEM. The number of publications per year was obtained by a PubMed search using the query 'correlative AND light AND electron AND microscopy AND fluorescence'. A clear rise is visible from the early 2000s, which coincides with crucial technical developments in the field of fluorescence microscopy.

With this approach, they were able to study the molecular and ultrastructural organization of myosin at the lamellum of fibroblasts. They continued to optimize this CLEM workflow and found that bipolar myosin filaments arranged parallel to each other, forming many long stack-like assemblies [11–13], something which was recently confirmed by novel super-resolution FM approaches [14,15]. The same CLEM workflow was further applied to study non-centrosomal microtubules in epithelial cells [16].

Further developments towards the end of the 1990s and the early 2000s were driven by the use of electron-dense small probes that were visible by both FM and EM without additional chemical or enzymatic reactions. These include the use of fluoro-nanogold probes [17,18] and quantum dots [19,20]. Fluoro-nanogold probes are composed of biomolecules (antibodies, streptavidin) that are coupled to extremely small nanogold particles (1.4 nm) as well as a fluorescent organic dye. Quantum dots are semiconductor particles that are intrinsically fluorescent and electron-dense. Due to their small size, fluoro-nanogold probes and quantum dots penetrate well into tissue sections [17–19] or flat biological samples prior to embedding [20], which make them very well suited for immunolabelling in fluorescence CLEM approaches. Despite the fact that these probes can be applied to address many different biological questions, their development did not lead to a significant rise in the application of CLEM in molecular and cell biology research. The increased popularity of fluorescence CLEM is set in motion by two other developments in fluorescence microscopy: (a) the discovery and engineering of fluorescent proteins (FPs) [21,22] and (b) the invention of super-resolution microscopy (SR) [23,24].

The introduction of fluorescent protein tags

Live cell imaging followed by EM sample preparation

The first renewed interest in fluorescence CLEM approaches for biological questions was spiked by the increased application of FPs for FM studies in the early 2000s. The use of FPs avoided the need for complex fixation and staining procedures for imaging the molecules of interest and CLEM approaches could now also address biological questions related to complex dynamic processes within cells. One of the first studies that applied FPs in a true CLEM approach came from the group of Alexander Mironov [25,26]. They used a VSVG-GFP reporter probe to first visualize the transport of vesicles from the Golgi to the plasma membrane by FM. The FM was performed on living cells and the dynamic information was used to determine the exact moment of fixation during fusion of the vesicles. To subsequently locate the VSVG-positive vesicles in the electron microscope, VSVG was indirectly labelled with HRP after fixation and the ultrastructure of the Golgi to plasma membrane vesicles during fusion could be studied [25,26].

Using the same rationale, the group of Judith Klumperman later optimized a workflow where live-cell FM was followed by immunolabelling of ultrathin cryosections for immuno-EM [27]. With this approach, they were able to study the dynamics of LAMP1-positive vesicles in cells that had taken up dextran. This dynamic information from the FM could then be correlated with the vesicle ultrastructure using EM. Around the same time, it was also shown that FP-based CLEM could be applied to entire organisms [28,29]. In these studies, tubulin or histone molecules were fluorescently tagged and used to determine the developmental stages of the nematode *Caenorhabditis elegans*. After fluorescence imaging, the animals were flash frozen at specific stages during development and the ultrastructure was studied by EM. Crucial for correlating the molecular localization by live-cell FM and the ultrastructure by EM is the time it takes to fix or freeze the sample. In contrast to chemical fixation, which can be done almost instantly during live cell imaging, transferring a sample to a flash or plunge freezer takes time. The development of a rapid transfer system, which enables freezing of the sample within 3 s after live cell imaging, has therefore also significantly contributed to the applicability of fluorescence CLEM approaches [30].

Preservation of FP fluorescence after fixation/embedding

So far, the work with FPs in fluorescence CLEM workflows was still limited by the fact that FM had to be performed before fixation or cryopreservation. The reason for this was that the FPs used for CLEM lost their ability to fluoresce after fixation and resin embedding due to protein denaturation. One of the first reports that demonstrated the retainment of GFP fluorescence in resins was published in 2003 [31]. In this study, a hydrophilic resin was used to embed chemically fixed zebrafish that expressed a GFP fusion protein. Retaining GFP fluorescence after resin embedding allowed the investigators to first locate a subset of rods in the fish retina before thin sectioning for EM ultrastructural analysis [31]. This greatly reduced the time to find appropriate regions of interest in tissue samples.

Since it is well established that chemical fixation creates many ultrastructural artefacts [32], subsequent protocols were developed for the preservation of GFP signal after cryofixation, freeze substitution and resin embedding. In the first approach, GFP-Caveolin3 was expressed in zebrafish and the animals were high pressure frozen and freeze substituted before microscopy analysis [33]. GFP fluorescence signal was still present and the molecular localization of caveolin by FM could be directly correlated with the ultrastructure of the plasma membrane by transmission EM. These initial protocols were later adapted and applied to study endocytosis in yeast cells [34–36]. For this work, proteins involved in endocytosis were fused to GFP or mCherry and expressed in yeast cells. Dual colour fluorescence microscopy combined with 3D electron tomography subsequently allowed for an ultrastructural analysis of endocytic vesicles [36]. An interesting additional observation that was useful for CLEM applications was that GFP retains fluorescence in-resin in vacuum, which allowed it to be studied in an integrated light and electron microscope [37].

Super-resolution CLEM

Resolution gap

Historically, the main problem for addressing appropriate biological questions for fluorescence CLEM has been the so-called 'resolution gap'. While the resolution of conventional FM is approximately 200 nm due to the diffraction of light, EM has a resolution that is about two orders of magnitude higher (~ 1 nm). This difference in resolution is referred to as the resolution gap and makes it hard to correlate the information that is derived from fluorescence and electron images. In other words, the uncertainty of the localization of specific molecules with respect to the precise ultrastructural details limits the interpretation of the correlation mostly to feature identification.

Interestingly, the first efforts to bridge the resolution gap are the result of a procedure that was already common for EM approaches, namely ultrathin cryosectioning [38]. By using ultrathin cryosections, the effective axial resolution of FM could be increased to ~ 50 nm, depending on the thickness of the section, which is about an order of magnitude more than the regular axial resolution in FM (~ 800 nm) [39]. This principle has been applied to evaluate the ultrastructure of lactoferrin-positive granules in neutrophils [17] as well as the structural details of transcription sites [40]. Despite these efforts, the most important development for decreasing the resolution gap has been the application of super-resolution (SR) FM of biological samples (Fig. 2). In 2006, two revolutionary papers described the development of photoactivated localization microscopy (PALM, [23]) and stochastic optical reconstruction microscopy (STORM, [24]) techniques that brought the resolution of FM down to ~ 10–20 nm. With these techniques at hand, it became possible to precisely pinpoint the localization of specific molecules within an ultrastructural context.

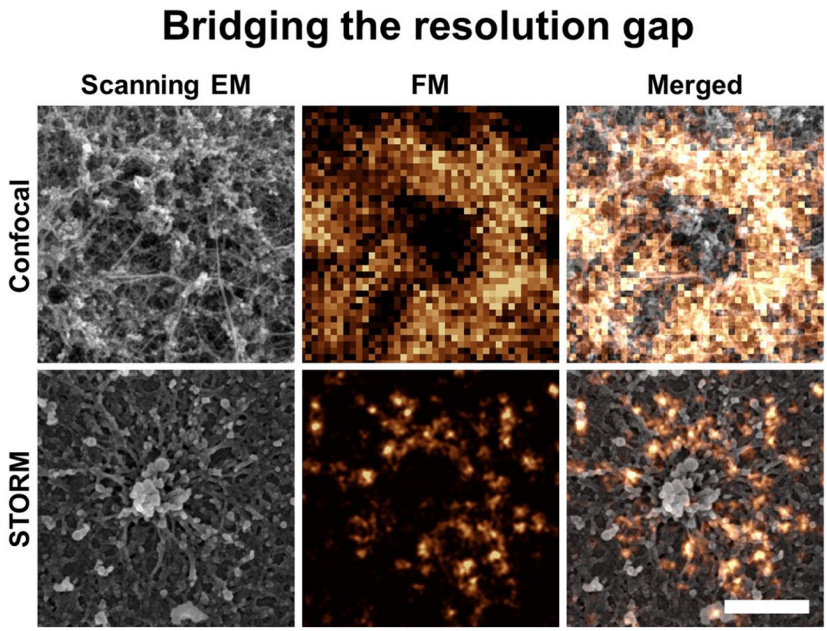

Fig. 2. Bridging the resolution gap. Shown are fluorescence CLEM images of the actin cytoskeleton in human immature dendritic cells. The FM signal visualizes the cytoskeletal adaptor molecule vinculin. The upper row shows an overlay of scanning EM with conventional confocal (resolution ~ 200 nm, obtained on a Zeiss LSM880 laser scanning confocal microscope (Carl Zeiss Microscopy, Oberkochen, Germany)) and the lower row shows an overlay with STORM (resolution ~ 20 nm, custom built STORM set-up at the Radboudumc Technology Center Microscopy). With STORM, molecular localization can be directly correlated with the ultrastructure of cellular structures. Scale bar = 500 nm.

SR-CLEM after 'classical' cryosectioning

Similar to the early fluorescence CLEM developments, the development of SR-CLEM went hand in hand with the developments in super-resolution FM. Already in the initial paper that describes the development of PALM super-resolution microscopy, an SR-CLEM workflow is applied [23]. In this particular case, transmission EM on Tokuyasu cryosections was used to confirm the nanometer resolution of PALM. By overlapping the fluorescence signal from mitochondria-targeted dEosFP using FM and the ultrastructure of mitochondria by EM, it could be demonstrated that PALM indeed has a nanometer scale resolution. Obviously, for this to work, the previously optimized workflows that allowed the preservation of FP fluorescence after aldehyde-based fixation and sectioning were instrumental. After the optimization of three-dimensional (3D) super-resolution microscopy techniques, a similar workflow was later applied to perform 3D SR-CLEM with interferometric PALM (iPALM) and focused ion beam (FIB) scanning EM [41]. In this work, the organization of the mitochondrial DNA-binding protein TFAM was studied in relation to the topology of the nucleoids and surrounding cristae. Since both iPALM and FIB-scanning EM are very specialized techniques, the same group also published a follow-up paper where they combined standard 2D PALM with SEM imaging on ultrathin (100 nm) cryosections [42]. Although this procedure cannot be used to study large volumes, the authors demonstrated its usefulness for a wide variety of biological structures including mitochondrial nucleoids, nuclear lamina and peroxisomes.

While aldehyde-fixed cryosections retain much of the fluorescence of photoswitchable or photoactivatable proteins, the ultrastructure is not well preserved [32]. Therefore, ongoing efforts try to optimize procedures for super-resolution microscopy that are compatible with the more commonly applied metallic oxide fixatives such as osmium tetroxide. The first successful workflow involved the use of low concentrations of osmium tetroxide and embedding of samples in glycidyl methacrylate resin [43]. In this study, PALM was performed on ultrathin sections and scanning EM was used for evaluating the ultrastructure. The authors used several FP fusion constructs that localized to different cellular compartments such as the nucleus and the mitochondria to demonstrate the wide potential of this approach. The resolution, however, of the PALM procedure was ~ 4–5 times lower as compared to optimal conditions due to the low photon count obtained from the osmium-fixed FPs.

An interesting solution to the problem of osmium-induced loss of photons came from a study that engineered FPs specifically for SR-CLEM applications [44]. For this work, the authors generated multiple variants of the photoconvertible FP mEos and identified several variants (mEos4a and mEos4b) that were relatively resistant to osmium-based fixation and resin embedding. As a proof of principle, the authors fused these mEos variants to several cellular components including the nuclear protein lamin A and showed that the localization precision of these novel mEos variants in resin was comparable to conventional mEos within osmium. Further engineering of mEos has recently even resulted in a variant (mEosEM) that survives embedding in Epon after osmium-based fixation, which was not the case for mEos4a/b, for improved SR-CLEM approaches [45].

Wet/dry protocols for SR-CLEM

Not all biological questions require the need to perform SR-FM after the sample has been prepared for EM. Especially in the case of membrane-bound structures, it can be beneficial to first perform the FM under hydrated conditions, which are optimal for maintaining fluorescence, and subsequently perform the EM on dried samples. Such an approach avoids the need of various optimization procedures and can use previously established CLEM procedures [46]. In particular, our understanding of clathrin-mediated endocytosis is greatly enhanced because of this type of SR-CLEM. To better understand clathrin-mediated endocytosis, a workflow was optimized that combined iPALM with platinum replica EM tomography of ventral plasma membrane preparations. This resulted in a comprehensive 3D map of the nanoscale organization of clathrin at clathrin-coated pits [47]. Later, this workflow was adapted to correlate the ultrastructure of clathrin-coated pits with antibody-based STORM imaging [48]. With this experimental set-up, the authors were able to study the localization of 19 different endocytic proteins during endocytosis and define the molecular architecture of endocytosis with nanometer precision. Comparable SR-CLEM workflows with hydrated SR-FM and subsequent scanning EM on dried samples were used to determine the nanoscale architecture of nuclear pores [49], HIV buds [50] and actin-based podosomes in immune cells [51].

Correlating cryo-SR with EM

The latest efforts in optimizing SR-CLEM have been focused on improving SR-FM imaging under

cryogenic conditions and correlating this to either cryo-electron tomography (ET) or other cryo-EM approaches. It is widely accepted that, for optimal preservation of the ultrastructure of biological samples, flash freezing is required. Yet, SR microscopy is extremely challenging under cryogenic conditions, mainly because of the requirement to use long-distance objectives with a relatively low numerical aperture. Despite these challenges, significant progress has been made for this type of cryo-correlative approaches, something we could call the current golden standard of CLEM. The first example of correlative cryo-PALM and cryo-electron tomography made use of photoactivatable GFP and investigated the nanoscale localization and molecular structure of a secretion protein system in bacteria [52]. Although the photon count of photoactivatable GFP was 5–10 times lower compared to optimal PALM (~ 200 photons per molecule resulting in a resolution of ~ 160 nm for the cryo-PALM), this work demonstrated the feasibility of this type of cryo-CLEM workflows. Not long after, it was shown that regular GFP could blink under cryogenic conditions and that a single molecule localization accuracy of ~ 40 nm could be achieved in biological samples [53]. By further adapting the procedure, a similar single molecular localization precision could be achieved under cryogenic conditions as compared to ambient temperatures [54].

One of the most impressive cryo-SR-CLEM efforts so far is presented in a recently published paper that combines cryogenic 3D single molecule localization microscopy with FIB scanning EM [55]. The vitrified samples were first evaluated using structured illumination microscopy (5 min per cell per colour) after which single molecule localization (1–2 days per cell per colour) was applied to a selected number of cells. Then, samples were freeze-substituted, resin embedded and imaged using FIB scanning EM (10–15 days per cell). In this study, mEmerald and Halo JF525 were found to be optimal for the FM imaging and several different proteins that localized to various intracellular compartment including the nucleus and peroxisomes were studied. Using this approach, the authors were able to find novel and unexpected features of virtually every marker they studied, suggesting CLEM approaches still hold great promise for the future [55].

Conclusions and outlook

As outlined above, although the first CLEM applications appeared over 40 years ago, the past decades have witnessed a rapid increase of scientific publications in which CLEM played a major role in unravelling molecular and cellular mechanisms. And while the future seems bright for SR-CLEM, a few hurdles need to be addressed in order to reach the full potential of CLEM (Fig. 3). Therefore, many aspects of this technique are still being developed or improved, including new or adjusted workflows, dedicated software, novel probes and novel combinations with other techniques.

Compared to FM, EM image acquisition is still relatively low-throughput and limited to small regions of interest, something which reduces the potential of CLEM applications. Because of this, improved set-ups for SR-CLEM aiming at increasing the image throughput and enlarging the correlation area are emerging. For example, a novel FIB/SEM technique based on a reactive oxygen source in a plasma FIB was combined with iPALM to image mitochondria in osteosarcoma cells and was shown to provide excellent 3D registration between the two different types of images [56]. For the plasma FIB, a rotating sample stage allowed

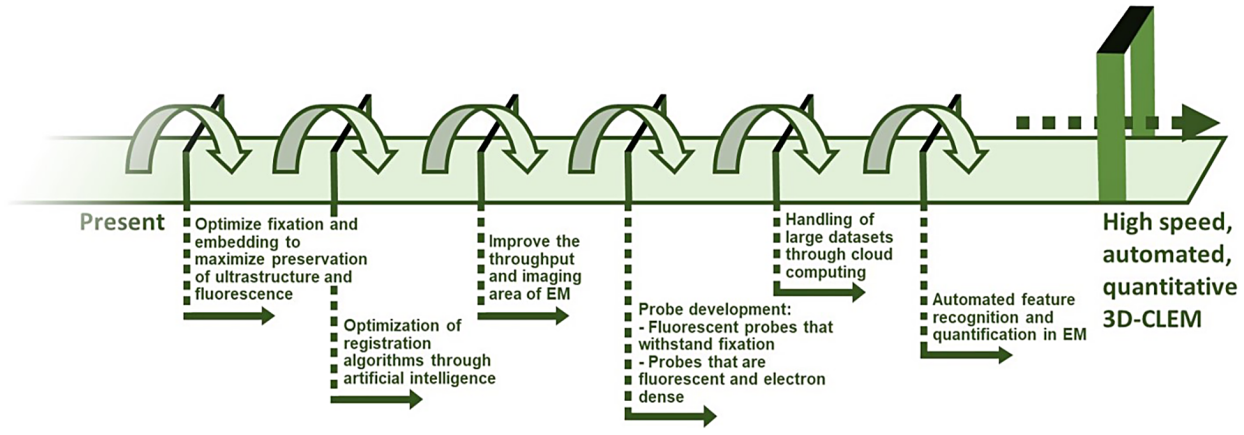

Fig. 3. Current challenges for fluorescence CLEM. See text for further details.

the 3D analysis of several hundreds of micrometer-large region of interest of resin-embedded human osteosarcoma cells through a process known as oxygen serial spin mill (OSSM). Compared to conventional FIB-SEM, OSSM/SEM offers consistent slice thickness, gentle erosion and better contrast without the need of a high dose of post-staining and fixation [56]. We anticipate that the combination of OSSM/SEM with other SR microscopy techniques will also be pursued to allow high-precision imaging of large areas.

Furthermore, although much progress has already been made in trying to solve the challenge of different sample preparation requirements between FM and EM, novel CLEM workflows are continuously being developed. For example, immuno-CLEM workflows based on TEM, SEM and scanning transmission EM (STEM) in combination with Tokuyasu sections and immunolabelling have recently been optimized to allow the identification of many cell markers and their relation to ultrastructural morphology in large sections of heterogeneous tissues [57]. While immuno-CLEM-TEM has mostly been used to identify subcellular structures, Oorschot et al. [57] provided a detailed comparison of the advantages of the three immune-CLEM approaches, which allowed the identification of tissue stem cells in whole zebrafish brain. More recently, a protocol was published for increasing the in-resin fluorescence of GFP [58]. This protocol refined previously established workflows using freeze substitution and Lowicryl HM20 embedding [37]. The continued efforts to improve the preservation of fluorescent signals after resin embedding are an important step towards future 3D-CLEM experiments.

While in-resin CLEM can simplify the correlation of EM and FM images, its application is also still relatively limited due to the low number of FPs/dyes that withstand CLEM processing. Therefore, besides fine-tuning protocols for retaining GFP fluorescence, we also expect the engineering and identification of other FPs as potential additional CLEM probes. For example, a study by Tanida et al. [59] resulted in the identification of mWasabi, variant-0 CoGFP and mCherry 2 as being relatively resistant to osmium treatment. This work showed that these FPs remained fluorescent in 100-nm thin sections of Epon-embedded cells, allowing two-colour in-resin CLEM of mitochondria and endoplasmic reticulum [59]. For SR-CLEM specifically, the development of fluorescent probes for multicolour imaging is even more challenging: indeed, SR-FM techniques such as PALM and STORM require fluorophore state conversions that need to be retained after sample preparation, something which has been achieved for only a few probes [44,45]. Moreover, the ultraviolet light that is commonly necessary to stimulate state conversions enhances glutaraldehyde-induced autofluorescence [60], further complicating the applicability of these FPs to CLEM.

The development or improvement of multimodal probes that are both fluorescent and electron dense is also a continuous quest in CLEM. These probes can be used to label specific components in a biological sample but can also act as fiducial landmarks to precisely overlay electron and fluorescent images. Fluorescent green colour-emitting nanodiamonds have been reported to resist exposure to electron beams, harsh chemical treatments, staining with heavy metal, maintaining their fluorescent properties fully intact for light microscopy [61]. Similarly, fluorescent nanoclusters composed of several atoms of platinum [62] or iridium-based luminescent metal complexes [63] exhibit electron density as well as fluorescence emission enabling highly accurate image registration. Very recently, surface-engineered ultrasmall and ultrabright gold nanoclusters have been used in stimulated emission depletion (STED) and CLEM allowing nanoscopic imaging of cellular tubulin [64].

Besides improving sample workflows and expanding chemical probes, considerable efforts are devoted to the design and optimization of dedicated software for CLEM. One of the most important aspects here is the improvement of image registration algorithms for overlaying FM and EM images. For this, most studies classically use so-called fiducials, which are markers that can be observed in both light and electron microscopy [34,65,66]. Alternatively, the holes in the EM grid itself can be used as spatial reference points [67]. In all cases, after image acquisition, semi-automated algorithms are used to identify the fiducials and transform the EM or FM image for the overlay. With the rise of artificial intelligence in image analysis, we foresee that, in the near future, image registration will be performed with the help of deep-learning algorithms, which should greatly facilitate CLEM processing. Other software-based developments facilitate automated and customizable cryo-FIB preparation protocols [68]. The need for this type of customized and versatile algorithms is expected to increase as CLEM is more and more used in combination with other approaches such as photonic chip-assisted CLEM, which enables multimodal total internal reflection fluorescence microscopy over large fields of view with high precision localization of the area of interest [69], or click-array tomography-CLEM, which combines super-resolution array tomography [70] with click chemistry and was recently used to visualize, track and

quantify azido-modified antimicrobial sphingolipids in bacteria [71].

Finally, we expect CLEM to become increasingly quantitative in the future. Although CLEM is still relatively qualitative as compared to approaches using FM only, several studies have already demonstrated the power of quantitative CLEM to reveal the nanoscale architecture of clathrin-coated pits [48]. Also, Klumperman and colleagues used quantitative, on-section CLEM to reveal the ultrastructural distribution of endogenous endosomal proteins in hundreds of organelles [72]. In line with these exciting novel approaches, Bäuerlein and Baumeister [73] recently discussed the intriguing possibility of exploiting cryo-CLEM, with conventional or SR-FM, to create cellular molecular atlases, paving the way to what they dubbed 'visual proteomics'. Important to note here is that processing CLEM data for quantitative analysis is extremely demanding for computer hardware since often hundreds of gigabytes to several terabytes of data are collected per data set [55,74]. Nevertheless, we expect that, in combination with workflows for 3D-CLEM [75–78], these developments will open up the possibilities to perform quantitative 3D cryo-CLEM of large tissue regions to establish fully optics-based top-down strategies to unravel cellular and molecular research questions.

Acknowledgements

The authors would like to thank Ben Joosten for the acquisition of the images shown in Fig. 2. We further thank the Radboud Technology Center Microscopy of the Radboudumc for the use of their facilities. This work was financially supported by intramural funding of the Radboudumc to AC and by an NWO KLEIN grant (OCENW.KLEIN.494) awarded to KD. We apologize to all authors whose work was not mentioned due to space limitations. Open access funding enabled and organized by ProjektDEAL. Open access funding enabled and organized by ProjektDEAL.

References

1 Bucana C, Hoyer LC, Hobbs B, Breesman S, McDaniel M, Hanna MG Jr. Morphological evidence for the translocation of lysosomal organelles from cytotoxic macrophages into the cytoplasm of tumor target cells. *Cancer Res*. 1976;**36**:4444–58.
2 Wouters CH, Koerten HK. Combined light microscope and scanning electron microscope, a new instrument for cell biology. *Cell Biol Int Rep*. 1982;**6**:955–9.
3 Eckert BS, Snyder JA. Combined immunofluorescence and high-voltage electron microscopy of cultured mammalian cells, using an antibody that binds to glutaraldehyde-treated tubulin. *Proc Natl Acad Sci USA*. 1978;**75**:334–8.
4 Amato PA, Unanue ER, Taylor DL. Distribution of actin in spreading macrophages: a comparative study on living and fixed cells. *J Cell Biol*. 1983;**96**:750–61.
5 Wouters CH, Koerten HK, Bonnet J, Daems WT, Ploem JS. Quantitative DNA measurements in an instrument combining scanning electron microscopy and light microscopy. *J Microsc*. 1986;**141**:41–53.
6 Rieder CL, Bowser SS. Correlative immunofluorescence and electron microscopy on the same section of epon-embedded material. *J Histochem Cytochem*. 1985;**33**:165–71.
7 Tokuyasu KT, Maher PA. Immunocytochemical studies of cardiac myofibrillogenesis in early chick embryos. I. Presence of immunofluorescent titin spots in premyofibril stages. *J Cell Biol*. 1987;**105**:2781–93.
8 Rupp G, Bowser SS, Mannella CA, Rieder CL. Naturally occurring tubulin-containing paracrystals in *Allogromia*: immunocytochemical identification and functional significance. *Cell Motil Cytoskeleton*. 1986;**6**:363–75.
9 Bowser SS, Travis JL, Rieder CL. Microtubules associate with actin-containing filaments at discrete sites along the ventral surface of *Allogromia reticulopods*. *J Cell Sci*. 1988;**89**(Pt 3):297–307.
10 Verkhovsky AB, Borisy GG. Non-sarcomeric mode of myosin II organization in the fibroblast lamellum. *J Cell Biol*. 1993;**123**:637–52.
11 Svitkina TM, Borisy GG. Correlative light and electron microscopy of the cytoskeleton of cultured cells. *Methods Enzymol*. 1998;**298**:570–92.
12 Svitkina TM, Verkhovsky AB, Borisy GG. Improved procedures for electron microscopic visualization of the cytoskeleton of cultured cells. *J Struct Biol*. 1995;**115**:290–303.
13 Verkhovsky AB, Svitkina TM, Borisy GG. Myosin II filament assemblies in the active lamella of fibroblasts: their morphogenesis and role in the formation of actin filament bundles. *J Cell Biol*. 1995;**131**:989–1002.
14 Beach JR, Bruun KS, Shao L, Li D, Swider Z, Remmert K, et al. Actin dynamics and competition for myosin monomer govern the sequential amplification of myosin filaments. *Nat Cell Biol*. 2017;**19**:85–93.
15 Hu S, Dasbiswas K, Guo Z, Tee YH, Thiagarajan V, Hersen P, et al. Long-range self-organization of cytoskeletal myosin II filament stacks. *Nat Cell Biol*. 2017;**19**:133–41.
16 Vorobjev IA, Svitkina TM, Borisy GG. Cytoplasmic assembly of microtubules in cultured cells. *J Cell Sci*. 1997;**110**(Pt 21):2635–45.
17 Takizawa T, Suzuki K, Robinson JM. Correlative microscopy using FluoroNanogold on ultrathin

cryosections. Proof of principle. *J Histochem Cytochem*. 1998;**46**:1097–102.
18 Takizawa T, Robinson JM. FluoroNanogold is a bifunctional immunoprobe for correlative fluorescence and electron microscopy. *J Histochem Cytochem*. 2000;**48**:481–6.
19 Nisman R, Dellaire G, Ren Y, Li R, Bazett-Jones DP. Application of quantum dots as probes for correlative fluorescence, conventional, and energy-filtered transmission electron microscopy. *J Histochem Cytochem*. 2004;**52**:13–8.
20 Giepmans BN, Deerinck TJ, Smarr BL, Jones YZ, Ellisman MH. Correlated light and electron microscopic imaging of multiple endogenous proteins using quantum dots. *Nat Methods*. 2005;**2**:743–9.
21 Chalfie M, Tu Y, Euskirchen G, Ward WW, Prasher DC. Green fluorescent protein as a marker for gene expression. *Science*. 1994;**263**:802–5.
22 Inouye S, Tsuji FI. Aequorea green fluorescent protein. Expression of the gene and fluorescence characteristics of the recombinant protein. *FEBS Lett*. 1994;**341**:277–80.
23 Betzig E, Patterson GH, Sougrat R, Lindwasser OW, Olenych S, Bonifacino JS, et al. Imaging intracellular fluorescent proteins at nanometer resolution. *Science*. 2006;**313**:1642–5.
24 Rust MJ, Bates M, Zhuang X. Sub-diffraction-limit imaging by stochastic optical reconstruction microscopy (STORM). *Nat Methods*. 2006;**3**:793–5.
25 Polishchuk RS, Polishchuk EV, Marra P, Alberti S, Buccione R, Luini A, et al. Correlative light-electron microscopy reveals the tubular-saccular ultrastructure of carriers operating between Golgi apparatus and plasma membrane. *J Cell Biol*. 2000;**148**:45–58.
26 Mironov AA, Polishchuk RS, Luini A. Visualizing membrane traffic in vivo by combined video fluorescence and 3D electron microscopy. *Trends Cell Biol*. 2000;**10**:349–53.
27 van Rijnsoever C, Oorschot V, Klumperman J. Correlative light-electron microscopy (CLEM) combining live-cell imaging and immunolabeling of ultrathin cryosections. *Nat Methods*. 2008;**5**:973–80.
28 Muller-Reichert T, Srayko M, Hyman A, O'Toole ET, McDonald K. Correlative light and electron microscopy of early *Caenorhabditis elegans* embryos in mitosis. *Methods Cell Biol*. 2007;**79**:101–19.
29 Muller-Reichert T, Mantler J, Srayko M, O'Toole E. Electron microscopy of the early *Caenorhabditis elegans* embryo. *J Microsc*. 2008;**230**:297–307.
30 Verkade P. Moving EM: the rapid transfer system as a new tool for correlative light and electron microscopy and high throughput for high-pressure freezing. *J Microsc*. 2008;**230**:317–28.
31 Luby-Phelps K, Ning G, Fogerty J, Besharse JC. Visualization of identified GFP-expressing cells by light and electron microscopy. *J Histochem Cytochem*. 2003;**51**:271–4.
32 Kellenberger E, Johansen R, Maeder M, Bohrmann B, Stauffer E, Villiger W. Artefacts and morphological changes during chemical fixation. *J Microsc*. 1992;**168**:181–201.
33 Nixon SJ, Webb RI, Floetenmeyer M, Schieber N, Lo HP, Parton RG. A single method for cryofixation and correlative light, electron microscopy and tomography of zebrafish embryos. *Traffic*. 2009;**10**:131–6.
34 Kukulski W, Schorb M, Welsch S, Picco A, Kaksonen M, Briggs JA. Correlated fluorescence and 3D electron microscopy with high sensitivity and spatial precision. *J Cell Biol*. 2011;**192**:111–9.
35 Kukulski W, Schorb M, Welsch S, Picco A, Kaksonen M, Briggs JA. Precise, correlated fluorescence microscopy and electron tomography of lowicryl sections using fluorescent fiducial markers. *Methods Cell Biol*. 2012;**111**:235–57.
36 Kukulski W, Schorb M, Kaksonen M, Briggs JA. Plasma membrane reshaping during endocytosis is revealed by time-resolved electron tomography. *Cell*. 2012;**150**:508–20.
37 Peddie CJ, Blight K, Wilson E, Melia C, Marrison J, Carzaniga R, et al. Correlative and integrated light and electron microscopy of in-resin GFP fluorescence, used to localise diacylglycerol in mammalian cells. *Ultramicroscopy*. 2014;**143**:3–14.
38 Tokuyasu KT. A technique for ultracryotomy of cell suspensions and tissues. *J Cell Biol*. 1973;**57**:551–65.
39 Robinson JM, Takizawa T, Pombo A, Cook PR. Correlative fluorescence and electron microscopy on ultrathin cryosections: bridging the resolution gap. *J Histochem Cytochem*. 2001;**49**:803–8.
40 Pombo A, Hollinshead M, Cook PR. Bridging the resolution gap: imaging the same transcription factories in cryosections by light and electron microscopy. *J Histochem Cytochem*. 1999;**47**:471–80.
41 Kopek BG, Shtengel G, Xu CS, Clayton DA, Hess HF. Correlative 3D superresolution fluorescence and electron microscopy reveal the relationship of mitochondrial nucleoids to membranes. *Proc Natl Acad Sci USA*. 2012;**109**:6136–41.
42 Kopek BG, Shtengel G, Grimm JB, Clayton DA, Hess HF. Correlative photoactivated localization and scanning electron microscopy. *PLoS One*. 2013;**8**: e77209.
43 Watanabe S, Punge A, Hollopeter G, Willig KI, Hobson RJ, Davis MW, et al. Protein localization in electron micrographs using fluorescence nanoscopy. *Nat Methods*. 2011;**8**:80–4.
44 Paez-Segala MG, Sun MG, Shtengel G, Viswanathan S, Baird MA, Macklin JJ, et al. Fixation-resistant photoactivatable fluorescent proteins for CLEM. *Nat Methods*. 2015;**12**:215–8, 4 p following 218.

45 Fu Z, Peng D, Zhang M, Xue F, Zhang R, He W, et al. mEosEM withstands osmium staining and Epon embedding for super-resolution CLEM. *Nat Methods*. 2020;**17**:55–8.
46 Collins A, Warrington A, Taylor KA, Svitkina T. Structural organization of the actin cytoskeleton at sites of clathrin-mediated endocytosis. *Curr Biol*. 2011;**21**:1167–75.
47 Sochacki KA, Shtengel G, van Engelenburg SB, Hess HF, Taraska JW. Correlative super-resolution fluorescence and metal-replica transmission electron microscopy. *Nat Methods*. 2014;**11**:305–8.
48 Sochacki KA, Dickey AM, Strub MP, Taraska JW. Endocytic proteins are partitioned at the edge of the clathrin lattice in mammalian cells. *Nat Cell Biol*. 2017;**19**:352–61.
49 Loschberger A, Franke C, Krohne G, van de Linde S, Sauer M. Correlative super-resolution fluorescence and electron microscopy of the nuclear pore complex with molecular resolution. *J Cell Sci*. 2014;**127**:4351–5.
50 Van Engelenburg SB, Shtengel G, Sengupta P, Waki K, Jarnik M, Ablan SD, et al. Distribution of ESCRT machinery at HIV assembly sites reveals virus scaffolding of ESCRT subunits. *Science*. 2014;**343**:653–6.
51 Joosten B, Willemse M, Fransen J, Cambi A, van den Dries K. Super-resolution correlative light and electron microscopy (SR-CLEM) reveals novel ultrastructural insights into dendritic cell Podosomes. *Front Immunol*. 2018;**9**:1908.
52 Chang YW, Chen S, Tocheva EI, Treuner-Lange A, Lobach S, Sogaard-Andersen L, et al. Correlated cryogenic photoactivated localization microscopy and cryo-electron tomography. *Nat Methods*. 2014;**11**:737–9.
53 Kaufmann R, Schellenberger P, Seiradake E, Dobbie IM, Jones EY, Davis I, et al. Super-resolution microscopy using standard fluorescent proteins in intact cells under cryo-conditions. *Nano Lett*. 2014;**14**:4171–5.
54 Liu B, Xue Y, Zhao W, Chen Y, Fan C, Gu L, et al. Three-dimensional super-resolution protein localization correlated with vitrified cellular context. *Sci Rep*. 2015;**5**:13017.
55 Hoffman DP, Shtengel G, Xu CS, Campbell KR, Freeman M, Wang L, et al. Correlative three-dimensional super-resolution and block-face electron microscopy of whole vitreously frozen cells. *Science*. 2020;**367**:eaaz5357.
56 Wang J, Randolph S, Wu Q, Botman A, Schardt J, Bouchet-Marquis C, et al. Reactive oxygen FIB spin milling enables correlative workflow for 3D super-resolution light microscopy and serial FIB/SEM of cultured cells. *Sci Rep*. 2021;**11**:13162.
57 Oorschot V, Lindsey BW, Kaslin J, Ramm G. TEM, SEM, and STEM-based immuno-CLEM workflows offer complementary advantages. *Sci Rep*. 2021;**11**:899.
58 Baatsen P, Gabarre S, Vints K, Wouters R, Vandael D, Goodchild R, et al. Preservation of fluorescence signal and imaging optimization for integrated light and electron microscopy. *Front Cell Dev Biol*. 2021;**9**:737621.
59 Tanida I, Furuta Y, Yamaguchi J, Kakuta S, Oliva Trejo JA, Uchiyama Y. Two-color in-resin CLEM of Epon-embedded cells using osmium resistant green and red fluorescent proteins. *Sci Rep*. 2020;**10**:21871.
60 Collins JS, Goldsmith TH. Spectral properties of fluorescence induced by glutaraldehyde fixation. *J Histochem Cytochem*. 1981;**29**:411–4.
61 Prabhakar N, Peurla M, Shenderova O, Rosenholm JM. Fluorescent and electron-dense green color emitting nanodiamonds for single-cell correlative microscopy. *Molecules*. 2020;**25**:25.
62 Tanner H, Hodgson L, Mantell J, Verkade P. Fluorescent platinum nanoclusters as correlative light electron microscopy probes. *Methods Cell Biol*. 2021;**162**:39–68.
63 Shewring JR, Hodgson L, Bryant HL, Bullough PA, Weinstein JA, Verkade P. Refining a correlative light electron microscopy workflow using luminescent metal complexes. *Methods Cell Biol*. 2021;**162**:69–87.
64 Yang H, Wu Y, Ruan H, Guo F, Liang Y, Qin G, et al. Surface-engineered gold nanoclusters for stimulated emission depletion and correlated light and electron microscopy imaging. *Anal Chem*. 2022;**94**:3056–64.
65 Fokkema J, Fermie J, Liv N, van den Heuvel DJ, Konings TOM, Blab GA, et al. Fluorescently labelled silica coated gold nanoparticles as fiducial markers for correlative light and electron microscopy. *Sci Rep*. 2018;**8**:13625.
66 Paul-Gilloteaux P, Heiligenstein X, Belle M, Domart MC, Larijani B, Collinson L, et al. eC-CLEM: flexible multidimensional registration software for correlative microscopies. *Nat Methods*. 2017;**14**:102–3.
67 Yang JE, Larson MR, Sibert BS, Shrum S, Wright ER. CorRelator: interactive software for real-time high precision cryo-correlative light and electron microscopy. *J Struct Biol*. 2021;**213**:107709.
68 Klumpe S, Fung HKH, Goetz SK, Zagoriy I, Hampoelz B, Zhang X, et al. A modular platform for automated cryo-FIB workflows. *Elife*. 2021;**10**:e70506.
69 Tinguely JC, Steyer AM, Øie CI, Helle ØI, Dullo FT, Olsen R, et al. Photonic-chip assisted correlative light and electron microscopy. *Commun Biol*. 2020;**3**:739.
70 Micheva KD, Smith SJ. Array tomography: a new tool for imaging the molecular architecture and ultrastructure of neural circuits. *Neuron*. 2007;**55**:25–36.
71 Peters S, Kaiser L, Fink J, Schumacher F, Perschin V, Schlegel J, et al. Click-correlative light and electron microscopy (click-AT-CLEM) for imaging and tracking

azido-functionalized sphingolipids in bacteria. *Sci Rep*. 2021;**11**:4300.
72 van der Beek J, de Heus C, Liv N, Klumperman J. Quantitative correlative microscopy reveals the ultrastructural distribution of endogenous endosomal proteins. *J Cell Biol*. 2022;**221**:e202106044.
73 Bäuerlein FJB, Baumeister W. Towards visual proteomics at high resolution. *J Mol Biol*. 2021;**433**:167187.
74 Xu CS, Hayworth KJ, Lu Z, Grob P, Hassan AM, García-Cerdán JG, et al. Enhanced FIB-SEM systems for large-volume 3D imaging. *Elife*. 2017;**6**:e25916.
75 Kremer A, Van Hamme E, Bonnardel J, Borghgraef P, GuErin CJ, Guilliams M, et al. A workflow for 3D-CLEM investigating liver tissue. *J Microsc*. 2021;**281**:231–42.
76 Gemin O, Serna P, Zamith J, Assendorp N, Fossati M, Rostaing P, et al. Unique properties of dually innervated dendritic spines in pyramidal neurons of the somatosensory cortex uncovered by 3D correlative light and electron microscopy. *PLoS Biol*. 2021;**19**: e3001375.
77 Hoffmann PC, Giandomenico SL, Ganeva I, Wozny MR, Sutcliffe M, Lancaster MA, et al. Electron cryo-tomography reveals the subcellular architecture of growing axons in human brain organoids. *Elife*. 2021;**10**:e70269.
78 Dalecka M, Sabo J, Backova L, Rosel D, Brabek J, Benda A, et al. Invadopodia structure in 3D environment resolved by near-infrared branding protocol combining correlative confocal and FIB-SEM microscopy. *Int J Mol Sci*. 2021;**22**:7805.